Electronic Structure: Metals, Half Metals, Insulators   James Tobin, Chairman

Applications of the NRL tight-binding method to magnetic systems

M. J. Mehl,[a)] D. A. Papaconstantopoulos, and I. I. Mazin
Center for Computational Materials Science, Naval Research Laboratory, Washington, DC 20375-5000

N. C. Bacalis
Theoretical and Physical Chemistry Institute, National Hellenic Research Foundation, Athens, Greece

W. E. Pickett
Department of Physics, University of California-Davis, Davis, California 95616

The NRL developed tight-binding method has been very successful in describing the properties of nonmagnetic elemental metals and semiconductors with accuracy comparable to first-principles methods. In this article we discuss extensions of the method to magnetic systems. We first show that the method correctly predicts equilibrium ground state structures, elastic constants, and phonon frequencies in ferromagnetic iron. We also show how the magnetic calculations can be extended to noncollinear systems, focusing on the electronic behavior of iron. © *2001 American Institute of Physics.* [DOI: 10.1063/1.1356031]

I. INTRODUCTION

Spin-dependent density functional theory (SDFT),[1] when coupled with an appropriate exchange-correlation functional,[2] provides an excellent framework for the first-principles study of magnetic systems. The original formulation of von Barth and Hedin[1] even included noncollinear magnetization. Unfortunately SDFT cannot be used to study large-scale magnetization because, in most practical formulations, the computational time scales with the cube of the number of atoms. In practice one can study systems containing on the order of 100 atoms or less. Thus large magnetic clusters and the motion of bulk domain walls is beyond the current capabilities of SDFT.

There has been extensive work showing that nonpolarized density functional theory (DFT) results can be used as a database to produce parametrized atomistic potentials which can be used to study large systems. Predominant among these is, of course, the embedded atom method[3,4] and its generalizations.[5] Extensions for magnetism can be made in the same fashion. For example, Krasko[6] has developed a semiempirical method for determining the magnetic energy in iron from a Stoner model. This allows one to use the same potentials for both magnetic and nonmagnetic systems.

While these parametrized atomistic models are extremely valuable, they are not based on quantum mechanics, but only fitted to a database of results which contains first-principles and/or experimental energies. Thus these models will fail unpredictably when one is calculating configurations which are not ''close'' to the fitted database.

Parametrized tight-binding (TB) methods, on the other hand, implicitly include quantum mechanical features. The TB method developed at the Naval Research Laboratory

(NRL-TB)[7] has been shown to accurately predict correct ground state structures, elastic constants, phonon frequencies, stacking fault energies,[8] surface energies, and vacancy formation energies in transition metals,[7] the heavier row IIIA metals,[9] carbon and silicon,[10] and lead.[11] This article presents an extension of the tight-binding method to magnetic systems, including noncollinear spins.[12]

II. EXTENSION OF THE TIGHT-BINDING METHOD TO MAGNETIC SYSTEMS

The formalism of the NRL-TB has been presented in detail elsewhere.[7] Here we note that it is a two-center nonorthogonal Slater–Koster[13] method with environmentally sensitive on-site parameters, and otherwise only discuss the changes needed to implement spin dependent polarization.

In collinear SDFT, the total energy of a system can be written as

$$E[n_\uparrow, n_\downarrow] = \sum_i \left[\varepsilon_{\uparrow i} f(\varepsilon_{\uparrow i} - \mu) + \varepsilon_{\downarrow i} f(\varepsilon_{\downarrow i} - \mu) \right]$$
$$+ G[n_\uparrow, n_\downarrow], \tag{1}$$

where $\varepsilon_{\uparrow i}$ and $\varepsilon_{\downarrow i}$ are the eigenvalues for the majority and minority spin states, respectively, $f(x)$ is a Fermi broadening function,[14] μ is the Fermi level, $n_\uparrow$ and $n_\downarrow$ are the electron densities of the majority and minority states, and $G[n_\uparrow, n_\downarrow]$ is the SDFT energy not included in the band structure sum. We eliminate the latter term by defining a potential shift

$$V_0 = G[n_\uparrow, n_\downarrow]/N, \tag{2}$$

where N is the total number of electrons in the system. We shift all of the eigenvalues and the Fermi level by V_0:

$$\varepsilon'_{\uparrow i} = \varepsilon_{\uparrow i} + V_0, \quad \varepsilon'_{\downarrow i} = \varepsilon_{\downarrow i} + V_0, \quad \text{and} \quad \mu' = \mu + V_0 \tag{3}$$

[a)]Electronic mail: mehl@dave.nrl.navy.mil

so that the total energy (1) becomes

$$E[n_\uparrow, n_\downarrow] = \sum_i \left[\varepsilon'_{\uparrow i} f(\varepsilon'_{\uparrow i} - \mu') + \varepsilon'_{\downarrow i} f(\varepsilon'_{\downarrow i} - \mu') \right]. \quad (4)$$

We assign the polarization dependence to the on-site terms, which are sensitive to the neighboring environment. We therefore define two ''densities,'' $\rho_\uparrow$ and $\rho_\downarrow$, for each atom:

$$\rho_{(\uparrow,\downarrow)i} = \sum_{j \neq i} \exp(-\lambda^2_{\uparrow,\downarrow} |\mathbf{R}_i - \mathbf{R_j}|) F(|\mathbf{R}_i - \mathbf{R_j}|), \quad (5)$$

where the $\lambda_{\uparrow,\downarrow}$ are to be fit, $\mathbf{R}_i$ is the position of atom i, and $F(R)$ is a cutoff function which vanishes for $R > R_{\text{cut}}$.[7] Here we set $R_{\text{cut}} = 16.5$ Bohr. These densities then control the on-site parameters for atom i by

$$h_{(\uparrow,\downarrow)\ell i} = a_{(\uparrow,\downarrow)\ell} + b_{(\uparrow,\downarrow)\ell} \rho^{2/3}_{(\uparrow,\downarrow)} + c_{(\uparrow,\downarrow)\ell} \rho^{4/3}_{(\uparrow,\downarrow)}$$
$$+ d_{(\uparrow,\downarrow)\ell} \rho^2_{(\uparrow,\downarrow)}, \quad (6)$$

where ℓ is the angular momentum of the orbital, and the various a, b, c, and d are fitting parameters. Here we restrict ourselves to $\ell = s$, p, or d. For nonmagnetic calculations ($n_\uparrow = n_\downarrow$) we average the above on-site parameters.

The two-center hopping and overlap parameters are kept spin-independent, and have the quadratic form used in Eq. (11) of Ref. 7. All of this leads to 106 parameters which are used to reproduce the volume and structural dependence of the electronic eigenvalues and total energies found in a database of first-principles results. For iron we used calculations from the ferromagnetic bcc phase and the nonmagnetic fcc and bcc phases. The method for determining the parameters is described in Ref. 7. The reliability of these parameters will be described below.

Pickett[12] has shown that the atomic moment approximation (AMA) to the noncollinear spin problem can be implemented in a parametrized tight-binding scheme. A general matrix element between the L ($= \ell, m$) orbital of atom i and the L' ($= \ell', m'$) orbital of atom j can be written as

$$h_{iL,jL'} = t_{iL,jL'} \sigma_0 - 1/2 \boldsymbol{\Delta}_{iL,jL'} \cdot \boldsymbol{\sigma}, \quad (7)$$

where σ is the Pauli spin matrices and $\boldsymbol{\Delta}_{iL,jL'}$ is the exchange splitting, which is assumed to be in the direction of the magnetic moment. We determine t and Δ from the spin-polarized tight-binding matrix elements above by aligning the spins, and hence all of the $\boldsymbol{\Delta}$, in the $\hat{z}$ direction. Then

$$t_{iL,jL'} = 1/2(h_{\uparrow iL,jL'} + h_{\downarrow iL,jL'}), \quad (8)$$

and the magnitude of the exchange splitting is just

$$\Delta_{iL,jL'} = 1/2(h_{\downarrow iL,jL'} - h_{\uparrow iL,jL'}). \quad (9)$$

Note that the spin polarization only affects the on-site part of the Hamiltonian (6), so Δ is diagonal.

III. APPLICATION TO IRON

The first-principles energies and electronic eigenvalues in our database were computed using the full-potential linearized augmented plane wave (LAPW) method[15,16] and the Perdew–Wang generalized gradient approximation for the exchange and correlation energy.[2] We also performed first-
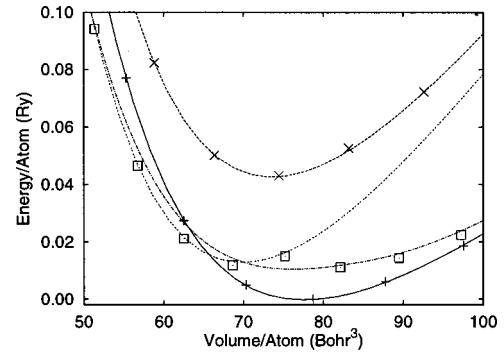

FIG. 1. Comparison of LAPW (points) and tight-binding calculations (lines) of the total energy of iron. The solid line is the ferromagnetic bcc phase. The dotted (highest) line is the nonmagnetic bcc phase. The other lines represent the TB ferromagnetic (—·—) and nonmagnetic (- - - -) fcc phases. The LAPW phases match the adjacent TB lines.

principles calculations for the hypothetical ferromagnetic fcc phase, but these were not included in the fit. In Fig. 1 we show the energy/volume behavior resulting from the fit. The interesting thing to note here is the behavior of fcc iron. First-principles calculations have shown that fcc iron has a high-spin and a low-spin (nearly nonmagnetic) solution. Our calculations show only the lowest energy phase as a function of volume. Note that our ferromagnetic TB calculations track the high-spin LAPW solution, while the nonmagnetic calculation tracks the low-spin LAPW solution.

We used the NRL-developed TB program ''STATIC'' [17] to calculate the elastic constants and some phonon frequencies of bcc iron at the equilibrium volume. These results are compared to experiment[18,19] in Table I. The agreement is impressive, since none of these calculations were included in the fit. This supports our belief that the tight-binding parameters are transferable to systems which are not included within the fit.

We plan to use the noncollinear spin theory of Sec. II to study the behavior of magnetic domain walls in iron. To this end, we present here a test case, using a two atom simple cubic supercell of bcc iron. One of the atoms in the unit cell has its spin vector aligned along the $\hat{z}$ axis, and we tilt the other atom so that its spin is at an angle θ to the $\hat{z}$ axis. Since we were only concerned with the behavior of the electronic structure, for these calculations we used a set of parameters which were fit to only ferromagnetic and nonmagnetic bcc iron. Figure 2 shows the resulting density of states when $\theta = (45°$ and $90°)$. Note the development of a pseudogap just below the Fermi level as θ increases. This gap becomes more pronounced as we approach the antiferromagnetic state ($\theta = 180°$).

TABLE I. Elastic constants (in GPa) and high-symmetry phonon frequencies (in cm^{-1}) of bcc ferromagnetic iron at the experimental lattice constant.

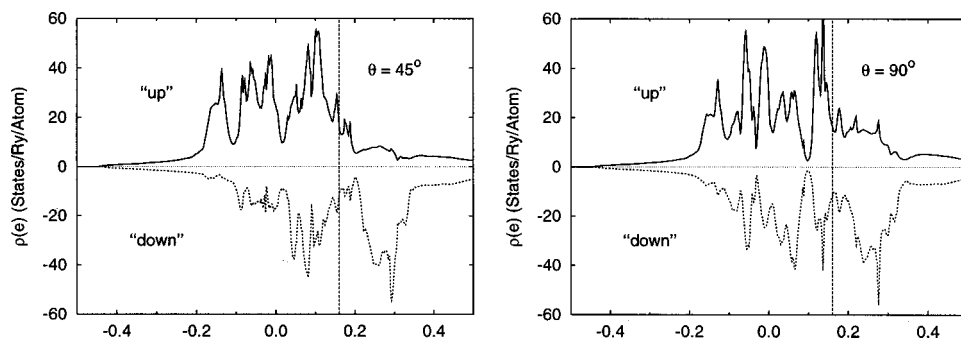|	Elastic constants		Phonon frequencies		
	TB	Exp. (Ref. 18)	**k** point	TB	Exp. (Ref. 19)
C_{11}	223	237	H	289	286
C_{12}	95	141	P	262	240
C_{44}	78	116			

FIG. 2. The electronic density of states for a two atom supercell of iron where one spin is in the ''up'' direction ($\hat{z}$) and the other is at an angle of θ. The ''up'' and ''down'' densities of state are projections relative to the $\hat{z}$ axis. The vertical line is the Fermi level.

IV. SUMMARY

We have shown that the NRL tight-binding method can be extended to handle both collinear and noncollinear spins. The method properly predicts the behavior of ferromagnetic fcc iron, including the low- and high-spin regions. In addition, the computed elastic constants and phonon frequencies have an accuracy comparable to those we found for nonmagnetic materials. Finally, we show that the method can be applied to noncollinear systems.

ACKNOWLEDGMENTS

[1] U. von Barth and L. Hedin, J. Phys. C **5**, 1629 (1972).
[2] J. P. Perdew, in *Electronic Structure of Solids '91*, edited by P. Ziesche and H. Eschrig (Akademie Verlag, Berlin, 1991), p. 11.
[3] A. F. Voter, in *Intermetallic Compounds: Principles and Applications*, edited by J. H. Westbrook and R. L. Fleischer (Wiley, London, 1994), Vol. 1.
[4] Y. Mishin, D. Farkas, M. J. Mehl, and D. A. Papaconstantopoulos, Phys. Rev. B **59**, 3393 (1999).
[5] M. I. Baskes, Phys. Rev. B **46**, 2727 (1992).
[6] G. L. Krasko, J. Appl. Phys. **79**, 4682 (1996).
[7] M. J. Mehl and D. A. Papaconstantopoulos, Phys. Rev. B **54**, 4519 (1996).
[8] M. J. Mehl, D. A. Papaconstantopoulos, N. Kioussis, and M. Herbranson, Phys. Rev. B **61**, 4894 (2000).
[9] S. H. Yang, M. J. Mehl, and D. A. Papaconstantopoulos, Phys. Rev. B **57**, R2013 (1998).
[10] N. Bernstein, M. J. Mehl, D. A. Papaconstantopoulos, N. I. Papanicolaou, M. Z. Bazant, and E. Kaxiras, Phys. Rev. B **62**, 4477 (2000).
[11] D. A. Papaconstantopoulos, M. J. Mehl, and B. Akdim, *Proceedings of the International Symposium on Novel Materials, Bhubaneswar, India, 1997*, edited by B. K. Rao (1998), pp. 393–403.
[12] W. E. Pickett, J. Korean Phys. Soc. (Proc. Suppl.) **29**, S70 (1996).
[13] J. C. Slater and G. F. Koster, Phys. Rev. **94**, 1498 (1954).
[14] M. J. Gillan, J. Phys.: Condens. Matter **1**, 689 (1989).
[15] O. K. Andersen, Phys. Rev. B **12**, 3060 (1975).
[16] S. H. Wei and H. Krakauer, Phys. Rev. Lett. **55**, 1200 (1985).
[17] For more information about the ''STATIC'' TB program, see http://cst-www.nrl.navy.mil/bind/dodtb/.
[18] G. Simmons and H. Wang, *Single Crystal Elastic Constants and Calculated Aggregate Properties: A Handbook*, 2nd ed. (MIT, Cambridge, MA, 1971).
[19] V. J. Minkiewicz, G. Shirane, and R. Nathans, Phys. Rev. **162**, 528 (1967).